

# Quantum state preparation of homonuclear molecular ions enabled via a cold buffer gas: An *ab initio* study for the $\text{H}_2^+$ and the $\text{D}_2^+$ case

S. Schiller\* and I. Kortunov

*Institut für Experimentalphysik, Heinrich-Heine-Universität Düsseldorf, 40225 Düsseldorf, Germany*

M. Hernández Vera and F. Gianturco

*Institut für Ionenphysik und Angewandte Physik, Universität Innsbruck, Technikerstrasse 25/3, 6020 Innsbruck, Austria*

H. da Silva, Jr.

*Laboratoire Aimé Cotton, CNRS/Université Paris-Sud/ENS Cachan, Orsay Cedex, France*

(Received 5 October 2016; revised manuscript received 24 January 2017; published 13 April 2017)

Precision vibrational spectroscopy of the molecular hydrogen ions is of significant interest for determining fundamental constants, for searching for new forces, and for testing quantum electrodynamics calculations. Future experiments can profit from the ability of preparing molecular hydrogen ions at ultralow kinetic energy and in preselected internal states, with respect to vibration, rotation, and spin degrees of freedom. For the homonuclear ions ( $\text{H}_2^+$ ,  $\text{D}_2^+$ ), direct laser cooling of the rotational degree of freedom is not feasible. We show by quantum calculations that rotational cooling by cold He buffer gas is an effective approach. For this purpose we have computed the energy-dependent cross sections for rotationally elastic and inelastic collisions,  $\text{h}_2^+(v=0, N) + \text{He} \rightarrow \text{h}_2^+(v=0, N') + \text{He}$  (where  $\text{h} = \text{H}, \text{D}$ ), using *ab initio* coupled-channel calculations. We find that rotational cooling to the lowest rotational state is possible within tens of seconds under experimentally realistic conditions. We furthermore describe possible protocols for the preparation of a single quantum state, where also the spin state is well defined.

DOI: [10.1103/PhysRevA.95.043411](https://doi.org/10.1103/PhysRevA.95.043411)

## I. INTRODUCTION

One of the outstanding challenges in the fields of few-body quantum physics and metrology is the achievement of ultrahigh-precision laser vibrational spectroscopy of the molecular hydrogen ion (MHI)  $\text{H}_2^+$ , a member of the family of one-electron molecules. These *ab initio* calculable systems at the intersection of atomic and molecular physics have enormous potential for ultraprecise spectroscopy at the  $10^{-17}$  fractional inaccuracy level [1,2]. So far, experiments have reached the  $10^{-9}$  level [3–5]. If a number of appropriately chosen rovibrational transitions of at least two of the three ions  $\text{H}_2^+$ ,  $\text{HD}^+$ ,  $\text{D}_2^+$  are determined, it is possible to test the accuracy of the *ab initio* calculations and to determine the values of the constants  $m_e/m_p$ ,  $m_p/m_d$ , charge radii of proton and deuteron, and the Rydberg energy [6]. Such determinations would be complementary to those performed on other systems and thus would provide an important consistency check, and could possibly lead to higher accuracy of the constants, and improved tests of their time independence.

The spectroscopy of  $\text{H}_2^+$  and  $\text{D}_2^+$  has been performed in several studies [7–12]. However, the techniques used so far do not promise to achieve fractional inaccuracies even at the level of present-day *ab initio* theoretical inaccuracies [13]. The challenge faced by methods of ultraprecise spectroscopy is the lack of accessible bound excited states in MHIs and that the homonuclear  $\text{H}_2^+$  and  $\text{D}_2^+$  lack electric-dipole-allowed rovibrational transitions. Therefore, a new suite of properly adapted manipulation techniques must be developed.

The charged nature of MHI enables their robust confinement in an ion trap and sympathetic laser cooling of their kinetic energy [14]. The preparation of MHIs in a single quantum state, the most suitable initial condition for ultrahigh-precision spectroscopy, is one of the necessary steps. For the heteronuclear  $\text{HD}^+$  molecule rotational laser cooling [15] and optical pumping [4], both on rovibrational transitions, can be used for this purpose. This is not possible for the homonuclear  $\text{H}_2^+$  and  $\text{D}_2^+$ , because of absence of spontaneous decay from rovibrational levels in the ground electronic state.

Suitable initial levels for future rovibrational precision spectroscopy [1,16] are, in particular, the two lowest-energy rovibrational states of  $\text{H}_2^+$  [ $(v=0, N=0)$  and  $(v=0, N=1)$ ], see Fig. 1. Here  $v$  denotes the vibrational quantum number and  $N$  is the rotational angular momentum quantum number. It has been proposed [17] to use state-selective photoionization of the neutral  $\text{H}_2$  [18], resulting in production of  $\text{H}_2^+$  predominantly in  $v=0, N=0, 1, \text{ or } 2$ , depending on the chosen laser excitation wavelength. This approach requires the use of a pulsed UV laser and appropriate experimental conditions (high density of neutral molecules).

In this paper we analyze an alternative approach to quantum state preparation, which is applicable to MHIs produced by standard electron-impact ionization. Here the ions are initially generated in a large number of rovibrational levels [17]. We propose to apply buffer gas cooling with cryogenic helium gas in order to relax the initial variety of internal states to the lowest-energy one. However, in homonuclear molecular ions having nuclear spin, the preparation in a *single* rotational state by cold buffer gas collisions is not possible in a straightforward way. We also propose approaches to resolve this limitation.

This paper is structured as follows: in Sec. II we recall key work done on cold He buffer gas cooling and give an overview

\*Corresponding author: [step.schiller@hhu.de](mailto:step.schiller@hhu.de)

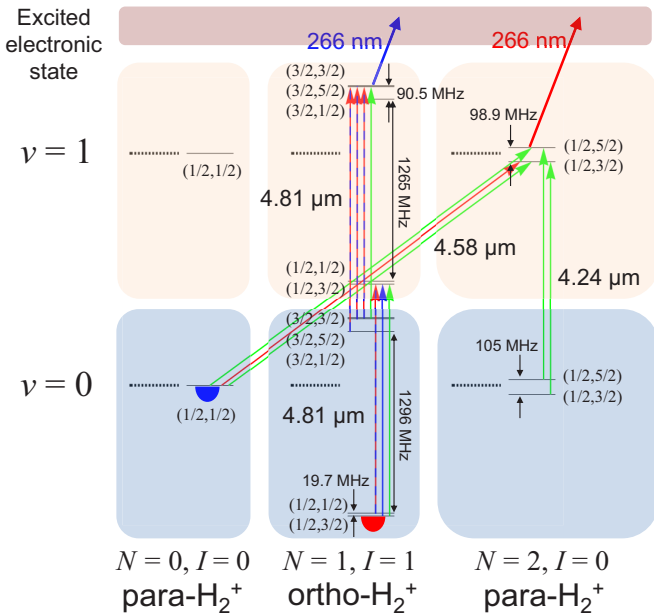


FIG. 1. The lowest rovibrational levels of  $\text{H}_2^+$  and their hyperfine structure, together with laser-induced electric quadrupole transitions considered for quantum state preparation and spectroscopy, after cooling by a buffer gas has occurred. Only the spin structure (spin-rotation and spin-spin) splittings [19] are to scale. Red arrows and blue-red dashed arrows: Transitions to be driven for preparation of a single ortho- $\text{H}_2^+$  quantum state (red semicircle); blue arrows and blue-red dashed arrows: transitions to be driven for preparation of a single para- $\text{H}_2^+$  quantum state (blue semicircle). Green arrows: Selected transitions with particularly small systematic effects, suitable for frequency metrology. Numbers in parentheses denote  $(F, J)$  (see text). Dashed lines: Level positions in absence of spin structure.

of the interactions that occur between MHIs and a He gas. In Sec. III we describe the method and results of our scattering calculations. In Sec. IV we apply the results for predicting the efficiency of rotational cooling. Section V is dedicated to a discussion of the feasibility of quantum state preparation. Section VI summarizes the findings.

## II. GENERAL CONSIDERATIONS

In the field of molecular ion spectroscopy, cold He buffer gas cooling in conjunction with ion trapping has been used successfully by several groups for many years [20–22], following initial studies with cold argon gas [23]. The rotational and vibrational cooling of molecules leads to a significantly reduced complexity of laser-induced rovibrational and electronic spectra, especially for polyatomic ions, enabling a deeper understanding of their structure and dynamical processes. The method was also applied to anions,  $\text{OH}^-$  [24] being a recent example.

Buffer gas cooling of  $\text{H}_2^+$ , however, has received only little experimental attention [25], and has not been used so far in connection with laser spectroscopy. A sophisticated variant of buffer gas cooling of molecular ions has been recently demonstrated, where the molecular ions are simultaneously translationally cooled by laser-cooled atomic ions (sympathetic cooling).  $\text{MgH}^+$  ions, sympathetically cooled by

laser-cooled  $\text{Ca}^+$  ions, were additionally rotationally cooled by He gas at 4 K, in a cryogenic trap. A rotational temperature of 7.5 K was reached in approximately 1 s of buffer gas interaction time [26], at a He gas density of  $10^{10} \text{ cm}^{-3}$ .

In analogy to this work, we shall consider here trapping MHIs in an ion trap of the linear quadrupole type, where the molecular ions are sympathetically cooled by co-trapped laser-cooled beryllium ions [14]. In contrast to the system of Ref. [26], in this case some of the trapped ions are *lighter* than or of equal mass as the buffer gas molecules ( $\text{H}_2^+$ ,  $\text{D}_2^+$  vs He). No experimental results on the effect of the buffer gas on the translational degrees of freedom of such trapped ions are known to us. Simulations of the interaction of trapped ions with buffer gas have been performed, albeit without including sympathetic cooling via ion-ion interactions [27–30]. These simulations do indicate that collisions with a buffer gas, in the presence of trap micromotion, can lead to ion translational heating, with steady-state ion temperature even above the gas temperature. The effect is reduced if the buffer gas has the same mass as the ion (e.g.,  $\text{D}_2^+$  and  $^4\text{He}$ ) or a smaller mass. The use of the light helium isotope  $^3\text{He}$  instead of  $^4\text{He}$  would lead to reduced heating for  $\text{D}_2^+$  and  $\text{H}_2^+$ , but would be a costly approach. However, based also on our own experimental study of collisional translational heating [31], and modeling of sympathetic cooling rates [32], we believe that the continuous sympathetic cooling of the MHIs by the laser-cooled atomic ions will, due to its strength, counteract any translational heating that the buffer gas may exert on the lighter trapped ions, at the low buffer gas densities, and hence low He atom-ion collision rates considered here.

In connection with rotational cooling, the issues of vibrational cooling and of competing reactions have to be considered first.

### A. Vibrational cooling

At 300 K thermal equilibrium,  $\text{H}_2^+$  is completely in the vibrational ground state  $v = 0$ . However, upon electron impact ionization,  $\text{H}_2^+$  is produced in a range of vibrational levels  $v$ . Levels  $v \leq 7$  occur with relative probabilities  $> 3\%$ , with approximately 40% of all ions being in  $v < 3$  [33,34]. No data or calculations on the rotational level distributions upon ionization are known to us. Theard and Huntress [25] observed that vibrational deactivation is possible by collisions with He at thermal energies. They found the reaction rates between  $0.1$  and  $0.5 \times 10^{-9} \text{ cm}^3/\text{s}$ , depending on  $v$ . At a He density  $n_{\text{He}} \simeq 7 \times 10^8 \text{ cm}^{-3}$  this leads to vibrational cooling times on the order of 10 s, an experimentally convenient time scale.

### B. Competing reactions

A first competing reaction is  $\text{H}_2^+ + \text{H}_2 \rightarrow \text{H}_3^+ + \text{H}$ . It occurs initially, during the ion generation step. The rate for this reaction is close to the Langevin rate  $\simeq 4.6 \times 10^{-10} \text{ cm}^3/\text{s}$  [28,35]. The reaction will lead to a loss of  $\text{H}_2^+$  ions and to an accumulation of  $\text{H}_3^+$  ions in the ion trap [32]. The loss can be compensated by starting with a sufficiently large number of neutral  $\text{H}_2$  molecules and by keeping their density small during ion generation, of order  $n_{\text{H}_2} \simeq 10^8 \text{ cm}^{-3}$ . In addition, in a cryogenic environment (necessary for cold He buffer gas cooling), the  $\text{H}_2$  gas is quickly removed by the pumping action

of the cryogenic surfaces of the apparatus, thereby bringing the reactions to a halt. The  $\text{H}_3^+$  ions accumulated in the trap can be ejected from it by an appropriate secular motion excitation technique.

A second competing reaction is the exothermic recombination channel  $\text{H}_2^+ + \text{He} \rightarrow \text{HeH}_2^+$ , forming a triatomic complex which supports several bound states. This reaction releases up to 0.35 eV. This could be a more serious issue, since it directly competes with the rotational cooling collisions. The reaction can occur via two different processes: (i) radiative association (where a photon is emitted). This has been found to have a negligible rate [36]. (ii) Ternary (nonradiative) association, where an additional collision partner satisfies overall momentum and energy conservation. The corresponding reaction rate is then proportional to  $(n_{\text{He}})^2$ . If the He gas density is kept sufficiently small, the rate of this reaction can also be kept small compared with the nonreactive (rotational/vibrational cooling) rates of interest here. Such ternary association reactions have recently been used to perform action spectroscopy of a rotational transition of  $\text{CD}^+$  [37] [ternary reaction rate of order  $10^{-30} \text{ cm}^6 \text{ s}^{-1} (n_{\text{He}})^2$ ]. The applicability of this technique to  $\text{H}_2^+$  and  $\text{D}_2^+$  is an interesting question deserving a separate study.

Finally, the reaction  $\text{H}_2^+(v) + \text{He} \rightarrow \text{HeH}^+ + \text{H}$  can occur. However, it is an endothermic reaction if  $v = 0, 1, 2$ , e.g., by 0.77 eV if  $v = 0$ . Thus, at the low collision energies of interest here, this reaction does not affect  $\text{H}_2^+$  in the ground vibrational level  $v = 0$ . The reaction is exothermic for vibrationally excited  $\text{H}_2^+(v \geq 3)$ , where  $v = 3$  requires additional rotational and/or translational energy) [25,38,39], with reaction rates (averaged over rotational states) in the range  $0.09$  to  $0.34 \times 10^{-9} \text{ cm}^3/\text{s}$  [25]. This implies that the vibrationally ( $v \geq 3$ ) excited MHIs produced during electron impact ionization will be destroyed if this is performed in the presence of He gas. This is acceptable and even desirable for the present purpose. The product  $\text{HeH}^+$  ions can subsequently be expelled from the ion trap. We point out that this reaction might also be of interest as a means of detecting a laser-induced vibrational excitation from the vibrational ground state (action spectroscopy). The excitation could, e.g., be a second (or higher) overtone electric quadrupole transition. The very small normalized excitation rate for such transitions rate would likely require a high-power laser source in order to achieve effective excitation.

Summarizing, if rotationally and vibrationally excited  $\text{H}_2^+$  molecules interact with He gas, vibrational deactivation and molecule loss occur, with similar time constants. However, in a cryogenic environment, the loss of  $\text{H}_2^+$  in the vibrational ground state is suppressed. This is expected to allow capturing and storing a sufficient number of  $\text{H}_2^+(v = 0)$  molecules in the trap. Therefore, the important questions are whether this vibrational deactivation can be followed by rotational deactivation *within* the vibrational ground state and what the characteristic cooling times are.

### III. SCATTERING CALCULATIONS

The simplicity of MHIs notwithstanding, the particular problem of scattering theory  $\text{He} + \text{MHI}(v, N) \rightarrow \text{He} + \text{MHI}(v', N')$  has, to the best of our knowledge, not been

treated before exactly. Scattering of He by other diatomic ions has been discussed before, e.g.,  $\text{Li}_2^+$  [40] and  $\text{MgH}^+$  [41,42]. The quantum analysis for MHIs is complicated by the presence of nonzero electron spin, but the solution has been obtained using the time-independent coupled-channel approach, including dynamical recoupling of angular momenta [43–45].

#### A. Symmetry considerations

$\text{H}_2^+$  molecules contain protons, which are fermions with nuclear spin  $I_p = 1/2$ . The molecules can have total nuclear spin  $I = 0$  (denoted by para- $\text{H}_2^+$ ) or  $I = 1$  (ortho- $\text{H}_2^+$ ). (The same distinction is well known for neutral  $\text{H}_2$ .) The para molecules have a spin wave function antisymmetric under proton exchange and therefore can only exist in rotational levels with even  $N$  (for which the rotational wave function is symmetric); ortho- $\text{H}_2^+$  molecules require odd  $N$  values.

The deuteron, a boson, has nuclear spin  $I_d = 1$ , hence the total nuclear spin of  $\text{D}_2^+$  can have the values  $I = 0, 1, 2$ . The total spin values  $I = 0, 2$  are associated with spin wave functions that are symmetric under exchange of the two identical nuclei. Hence, this case is called ortho- $\text{D}_2^+$ . Because the deuterons are bosons, the total molecular wave function must be *symmetric* under nucleus exchange and this requires that the rotational state be of *even*  $N$ . (Note that for  $\text{H}_2^+$ , the  $N = 0$  level instead occurs for para- $\text{H}_2^+$ , because protons are fermions.)  $\text{D}_2^+$  with  $I = 1$  is denoted by para- $\text{D}_2^+$  (antisymmetric spin wave function) and is associated with odd- $N$  rotational states (antisymmetric rotational wave function). (The same distinction holds for neutral  $\text{D}_2$ .)

In collisions with nonmagnetic particles such as He, the total nuclear spin  $I$  is conserved and para and ortho molecules do not interconvert. Therefore, in collisions, only rotational quantum number changes  $\Delta N = N - N' = 0, \pm 2, \pm 4, \dots$  are allowed.

#### B. Methods

The *ab initio* calculation requires as input the *ab initio* potential energy surface (PES) for the  $\text{He} + \text{MHI}(v, N)$  system. Recent high-level *ab initio* calculations, using a state-of-the-art multireference configuration interaction approach that included all single and double excitations, computed the PES [39]. Specifically, for the interaction potential of the He-h-h<sup>+</sup> complex (where h denotes H or D) we used the  $M = 8$  fitting choice using FCI/cc-pVQZ level for the basis set expansion [39]. From the potential in chemical coordinates  $V_{M8}(R_1, R_2, R_3)$ , we generated the subreactive potential of the initial collision state  $\text{He} + \text{h}_2^+(v, N)$  in Jacobi coordinates  $V_{M8}(r|R, \theta)$ .  $R$  is the distance of the He atom from the center of mass of the MHI,  $\theta$  is the angle between He atom position vector and the MHI axis, and  $r$  is the distance between the H or D atoms. Here we limit ourselves to MHIs in the ground vibrational level  $v = 0$ . The detailed features of the potential are analyzed elsewhere [46]. Multipolar coefficients up to  $\lambda = 20$  were included. They were obtained from the full three-dimensional PES by averaging over the ground-state vibrational wavefunction of the molecule.

### 1. The $\text{H}_2^+$ case

We solved the coupled-channel equations using a quantum scattering computer code developed by one of the present authors [47] and computed the elastic  $(0, N) \rightarrow (0, N' = N)$  and state-changing  $(0, N) \rightarrow (0, N' \neq N)$  cross sections as a function of collision energy up to  $4000 \text{ cm}^{-1}$ . The number of rotational states ( $N$  values) included in the asymptotic expansion of target states was checked for convergence by having all the open channels included plus at least two closed channels above each energy threshold as part of the full expansion of the coupled-channel wave function. The partial integral cross sections, depending on the total angular momentum of the system, have been carefully checked for convergence against the basis set size and propagator parameters and found to be well within 1%. In particular, we have propagated the solution from  $R = 0.1 \text{ nm}$  to  $R = 5 \text{ nm}$  with 500 steps of the Variable-Phase propagator [47]. The convergence of the sums on the partial cross sections to obtain the corresponding state-to-state integral cross sections was also controlled by extending the  $J$  values up to at least  $J_{\text{max}} = 80$ . The reliability index for our computed cross sections is around 1%–2%.

For para- $\text{H}_2^+$  we performed exact scattering calculations, including the electron-spin-rotation coupling  $\mathbf{s}_e \cdot \mathbf{N}$ . We repeated them by treating the molecule as a pseudo- $\Sigma$  system (i.e., ignoring electron spin and therefore ignoring the spin-rotation coupling). We compared the cross sections for both cases (summed over the spin states in the exact treatment) and found that they agree within 20%, mostly within 10% [46]. Thus, the spin dependence of the cross sections can be neglected for the present purpose.

For the more complicated case of ortho- $\text{H}_2^+$  (where electron-spin–nuclear-spin coupling is present in addition), we have also performed exact calculations. We found an even better agreement between the summed exact and the spinless cross sections. Therefore, in the following we use the latter. Details will be reported elsewhere [46].

### 2. The $\text{D}_2^+$ case

The PES does not depend on the mass of the hydrogen isotope, therefore the calculations for  $\text{D}_2^+$  are performed using the same PES as for  $\text{H}_2^+$ . We have not taken into account the spins, since the  $\text{H}_2^+$  case indicates that their effect is small.

### C. Rate coefficients of inelastic collisions

Rate coefficients  $k(T)$  are computed, for a given collisional temperature  $T$ , from the cross sections by an integration over the collision energy, with a temperature-dependent kernel. The collisional temperature is related to, but not identical to, the temperature of the He buffer gas. In the absence of micromotion of the ions, consideration of the center-of-mass motion of the collision partners leads to

$$T = \frac{m_{\text{He}} T_{\text{ion}} + m_{\text{ion}} T_{\text{He}}}{m_{\text{He}} + m_{\text{ion}}}. \quad (1)$$

Figure 2 shows a subset of the  $\text{H}_2^+$  inelastic scattering coefficients for the rotational levels relevant to this study (for additional coefficients, see: [48]). Rotational excitation

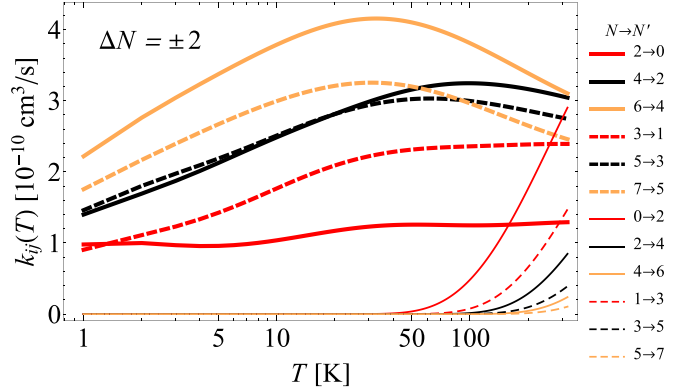


FIG. 2. Rate coefficients  $k_{i,j}(T)$  for rotational deexcitation  $N \rightarrow N - 2$  and rotational excitation  $N \rightarrow N + 2$ . Full lines: para- $\text{H}_2^+$ , dashed lines: ortho- $\text{H}_2^+$ .  $\Delta N = N - N'$ .

processes  $N \rightarrow N' > N$  are seen to be energetically suppressed at low temperature, since the kinetic collision energy is insufficient for providing the difference in rotational energy between final and initial level, amounting to  $42 \text{ K} \times [N'(N' + 1) - N(N + 1)]$ . The deexcitation rates for  $N \rightarrow N - 2$  are larger than the rates for  $N \rightarrow N - 4$  [46]. For excitation, the difference is a factor 10 or more.

Figure 3 shows some rate coefficients for  $\text{D}_2^+$ .

### D. Rate coefficients of elastic collisions

For  $\text{H}_2^+$  we show in Fig. 4 the rates for elastic collisions  $N \rightarrow N' = N$ . At, e.g.,  $T = 10 \text{ K}$ , the elastic rates for  $N = 0 \rightarrow 0$  and  $N = 1 \rightarrow 1$  are approximately 10 and 6 times larger than the deexcitation rates  $N = 2 \rightarrow 0$  and  $N = 3 \rightarrow 1$ . For  $\text{D}_2^+$  the elastic rates are presented in Fig. 5.

## IV. COOLING DYNAMICS

### A. Method

The rate coefficients allow computing the cooling dynamics using simple rate equations. They read  $d\mathbf{p}(t)/dt = n_{\text{He}} \mathbf{K}(T) \cdot \mathbf{p}(t)$ , with the fractional rotational populations

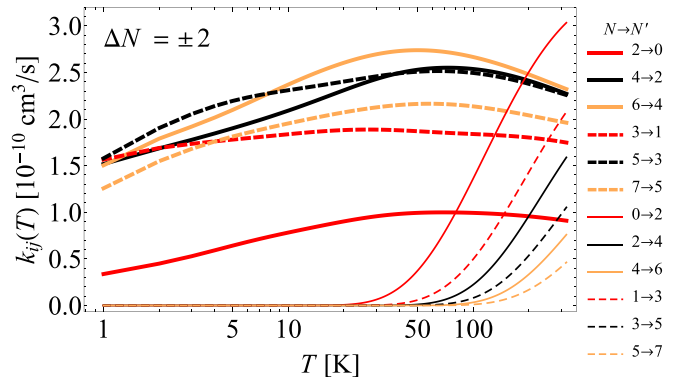


FIG. 3.  $\text{D}_2^+$  rate coefficients  $k_{i,j}(T)$  for rotational deexcitation  $N \rightarrow N - 2$  and rotational excitation  $N \rightarrow N + 2$ . Full lines: ortho- $\text{D}_2^+$ , dashed lines: para- $\text{D}_2^+$ .  $\Delta N = N - N'$ .

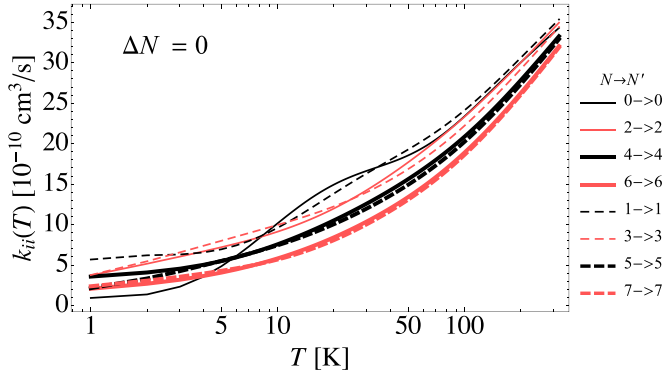


FIG. 4.  $\text{H}_2^+$  rate coefficients for rotationally elastic collisions  $N \rightarrow N'$ , as a function of collisional temperature. Full lines: para- $\text{H}_2^+$ , dashed lines: ortho- $\text{H}_2^+$ .  $\Delta N = N - N'$ .

$\mathbf{p}(t) = (p_1(t), p_2(t), \dots, p_{n-1}(t), 1 - \sum_{i=1}^{n-1} p_i(t))$ , and

$$\mathbf{K} = \begin{pmatrix} -\sum_{i=2}^n k_{1,i} & k_{2,1} & \dots & k_{n,1} \\ k_{1,2} & -\sum_{i=1, \neq 2}^n k_{2,i} & & \vdots \\ \vdots & & & \\ k_{1,n} & \dots & & -\sum_{i=1}^{n-1} k_{n,i} \end{pmatrix},$$

where  $i$  is an index corresponding to a particular rotational level  $N$ , and  $k_{i,j} = k_{i,j}(T)$  are the inelastic rate coefficients from level  $i$  to level  $j$ . The cases of ortho- and para- $\text{H}_2^+$  are treated separately, since interconversion is absent over the considered time scales.

The initial conditions  $p_i(t=0)$  and the gas temperature  $T_{\text{He}}$  must be chosen according to experimental considerations. He gas temperature as low as 4 K can be reached by standard techniques in cryogenic ion traps. MHIs sympathetically cooled by laser-cooled beryllium ions exhibit residual kinetic energy which is mostly micromotion energy. Its magnitude can be of order  $k_B \times (1 \text{ K})$ , if a large number of MHI is simultaneously trapped. If a single molecular ion is trapped and advanced laser cooling techniques are applied, the energy can be much less. The micromotion is not of thermal character. However, according to Eq. (1) we can neglect its effect if we assume a comparatively large collisional temperature,

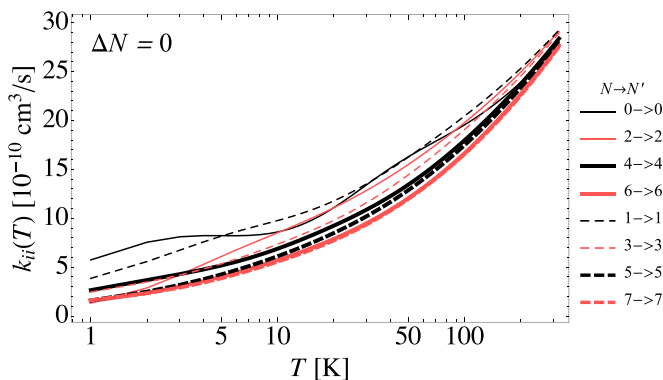


FIG. 5.  $\text{D}_2^+$  rate coefficients for rotationally elastic collisions  $N \rightarrow N'$ , as a function of collisional temperature. Full lines: ortho- $\text{D}_2^+$ , dashed lines: para- $\text{D}_2^+$ .

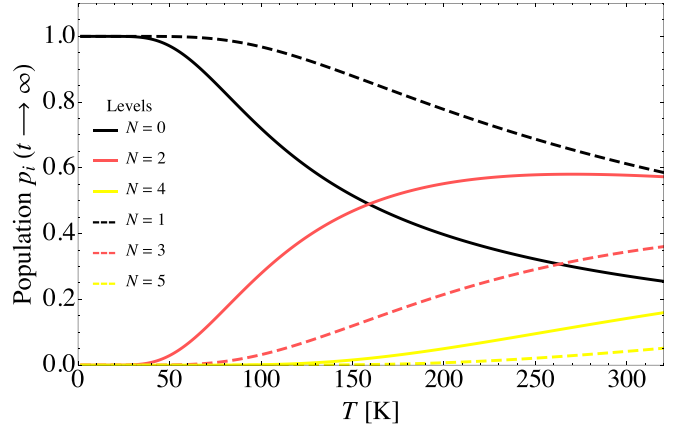


FIG. 6. Steady-state solution of the rate equations for rotational cooling of  $\text{H}_2^+$ , as a function of collisional temperature. Ortho and para subensembles are treated independently.

$T \geq 10 \text{ K}$ . The He gas temperature is  $T_{\text{He}} = 3 \text{ T}$  for  $\text{H}_2^+$  (2 T for  $\text{D}_2^+$ ), if the ion temperature can be neglected. In the calculations,  $T$  is kept constant in time since we assume that the He gas acts as a thermostat.

As mentioned above,  $\text{H}_2^+$  ions produced by electron impact ionization occur in a large range of rotational and vibrational states. Ortho- and para- $\text{H}_2^+$  will both be present. Collisions with He (even at  $T_{\text{He}} = 300 \text{ K}$ ) will relax the vibrationally excited levels to the vibrational ground state  $v=0$  and also reduce the rotational temperature. For the purpose of showing the feasibility of buffer gas cooling we nevertheless assume a high initial rotational temperature  $T_{\text{rot}} = 1000 \text{ K}$  and set the values  $p_i(t=0)$  according to the corresponding Boltzmann distribution. It is sufficient to consider  $n = 6$  levels for both para- $\text{H}_2^+$  and ortho- $\text{H}_2^+$ . We include processes with  $|\Delta N| \leq 10$ . For  $\text{D}_2^+$ , for simplicity, we restrict the number of initially populated rotational levels to the same as for the  $\text{H}_2^+$  simulations. Therefore, in this case the calculations were done with the initial condition  $T_{\text{rot}} = 500 \text{ K}$ .

## B. Results

### 1. Steady-state solution

The steady-state solution  $p_i(t \rightarrow \infty)$  of the rate equations is found upon setting  $d\mathbf{p}(t)/dt = 0$  and solving the resulting algebraic equations. Figure 6 shows the result for  $\text{H}_2^+$  and for different values of  $T$ . We verified that these steady-state population fractions for each nuclear spin subsystem indeed correspond to a Boltzmann distribution with  $T_{\text{rot}} = T$ . We find that the steady-state population fraction in the lowest rotational state for para- $\text{H}_2^+$  exceeds 95% if  $T < 50 \text{ K}$  while for ortho- $\text{H}_2^+$  this occurs if  $T < 100 \text{ K}$ . The result is independent of the helium density  $n_{\text{He}}$ , since  $d\mathbf{p}/dt$  is proportional to it. From an experimental point of view, such collisional temperatures (and consequently, He gas temperatures) represent a modest requirement which can be easily met. This is owed to the large rotational constant of  $\text{H}_2^+$ ,  $29.1 \text{ cm}^{-1}$  (41.9 K).

The result for  $\text{D}_2^+$  is shown in Fig. 7. Note that the collisional temperature required for cooling 95% of the ortho- $\text{D}_2^+$  ions into  $N=0$  is 30 K, and 50 K for the para- $\text{D}_2^+$  ions into  $N=1$ . These lower values compared to  $\text{H}_2^+$  (but

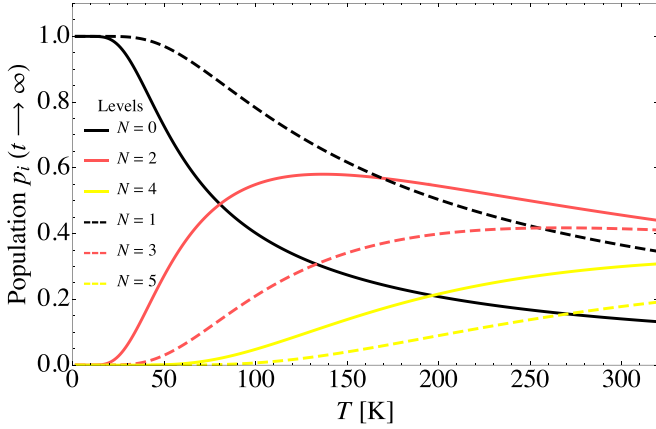


FIG. 7. Steady-state solution of the rate equations for rotational cooling of  $D_2^+$ , as a function of collisional temperature. Ortho and para subensembles are treated independently.

still easily reachable experimentally) are due to the two times smaller rotational constant of  $D_2^+$ .

## 2. Time dependence

Figure 8(a) shows an example of the time dependence of the cooling, for one particular value  $T$  and density  $n_{\text{He}}$ . Figure 8(b) shows the overall time evolution of the rotational energy content. We may define a characteristic time constant  $\tau$  by  $\langle E_{\text{rot}} \rangle(\tau) - \langle E_{\text{rot}} \rangle(t = \infty) = (\langle E_{\text{rot}} \rangle(t = 0) - \langle E_{\text{rot}} \rangle(t = \infty))/e$ , where  $\langle E_{\text{rot}} \rangle$  is the level-averaged rotational energy. Because  $d\mathbf{p}/dt$  is proportional to  $n_{\text{He}}$ , at fixed temperature  $\tau$  is inversely proportional to  $n_{\text{He}}$ . The product  $\tau \times n_{\text{He}}$  changes moderately with decreasing collisional temperature from  $3 \times 10^9$  to  $5 \times 10^9$  s/cm $^3$ , see Fig. 8(c). We note that  $\tau$  also depends weakly on the assumed initial rotational temperature, because the time evolution of  $\langle E_{\text{rot}} \rangle(t)$  is not a simple exponential but a superposition of different exponentials.

The rotational cooling process for  $D_2^+$  is shown in Fig. 9. Because of the similarity of the rate coefficients of  $D_2^+$  and  $H_2^+$ , also the characteristic time for  $D_2^+$  is similar to that for the  $H_2^+$  case.

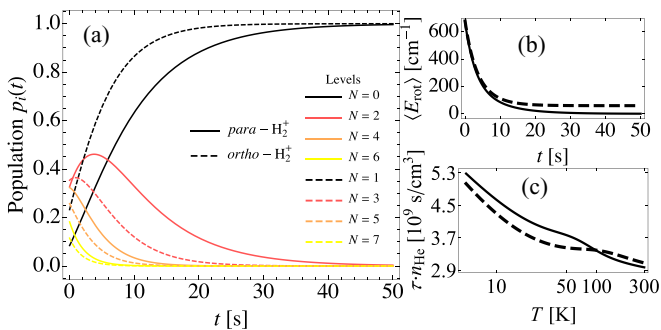


FIG. 8. (a) Time-dependent solution of the rate equations for rotational cooling of  $H_2^+$  at a helium density  $n_{\text{He}} = 1 \times 10^9 \text{ cm}^{-3}$ , collisional temperature  $T = 20 \text{ K}$ , and initial rotational temperature  $T_{\text{rot}} = 1000 \text{ K}$ . (b) The time dependence of the average rotational energy per  $H_2^+$  molecule  $\langle E_{\text{rot}} \rangle(t)$ . (c) The temperature dependence of  $\tau \times n_{\text{He}}$ , where  $\tau$  is the characteristic time of the rotational cooling.

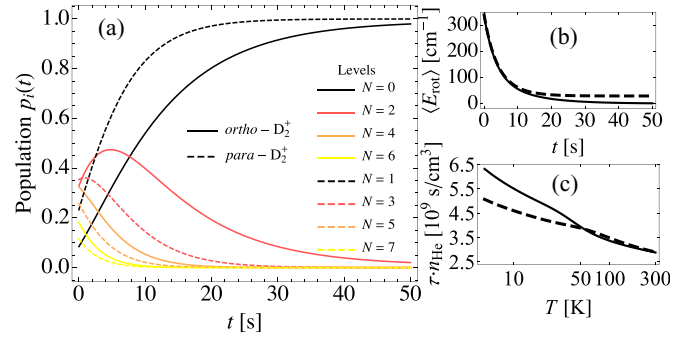


FIG. 9. (a) Time-dependent solution of the rate equations for rotational cooling of  $D_2^+$  at a helium density  $n_{\text{He}} = 1 \times 10^9 \text{ cm}^{-3}$ , collisional temperature  $T = 20 \text{ K}$ , and initial rotational temperature  $T_{\text{rot}} = 500 \text{ K}$ . (b) The time dependence of the average rotational energy per  $D_2^+$  molecule  $\langle E_{\text{rot}} \rangle(t)$ . (c) The temperature dependence of  $\tau \times n_{\text{He}}$ , where  $\tau$  is the characteristic time for cooling.

## 3. Operating conditions

The rate coefficient  $k$  for the  $N = 2 \rightarrow N' = 0$  and  $N = 3 \rightarrow N' = 1$  deexcitations at  $T = 10 \text{ K}$  are  $(1, 1.6) \times 10^{-10} \text{ cm}^3/\text{s}$ . At this collisional temperature,  $\tau \times n_{\text{He}} \approx 4.5 \times 10^9 \text{ s/cm}^3$ . Thus, over the time  $\tau$  the probability for such an energy-relaxing collision to occur is  $k_{N=2(3), N'=N-2}(10 \text{ K})(\tau \times n_{\text{He}})(10 \text{ K}) \approx 0.5 (0.7)$ . This implies that the actual time scale for achieving cooling to the steady-state  $\tau_c$  should conservatively be taken one order larger. This ensures that the rotational relaxation has fully occurred, i.e.,  $k_{N=2(3), N'=N-2}(10 \text{ K})(\tau_c \times n_{\text{He}})(10 \text{ K}) \gg 1$ .

In an experiment aimed for precision spectroscopy of  $H_2^+$  it would be desirable to use density values  $n_{\text{He}}$  so low that the mean time between (elastic plus inelastic) collisions with He is larger than the spectroscopy cycle time  $t_{\text{cycle}}$ . Thus,  $n_{\text{He, upper}} = 1/[k_{\text{tot}}(T) t_{\text{cycle}}]$ , where  $k_{\text{tot}}(T)$  is the total collision rate coefficient in the ground rotational state. Assuming the ideal gas behavior for He (i.e., thermal equilibrium with the cryostat cold enclosure), the corresponding upper limit for the pressure is  $p_{\text{He, upper}} = k_B T_{\text{He}} n_{\text{He, upper}}$ . For  $T = 10 \text{ K}$ , at the end of rotational cooling the elastic collisions by far dominate (compare Figs. 2 and 4), so that  $k_{\text{tot}}(T) = k_{N=0, N'=0}(T)$  or  $k_{N=1, N'=1}(T)$  for para or ortho species, respectively. If  $t_{\text{cycle}} = 1 \text{ s}$ , we find for both  $H_2^+$  and  $D_2^+$   $n_{\text{He, upper}} \simeq 1 \times 10^9 \text{ cm}^{-3}$  and therefore  $p_{\text{He, upper}} \simeq 4 \times 10^{-9} \text{ mbar}$ .

Experimentally, a viable approach could be to first perform the buffer gas rotational cooling, and then to pump out the He gas, effectively reducing collision rates strongly. In absence of collisions, the MHIs will not heat up again by any obvious mechanism. We point out that black-body radiation as a driving force for rotational heating is here ruled out, because black-body radiation essentially does not interact with homonuclear molecules and is weak due to the cryogenic environment.

## V. QUANTUM STATE PREPARATION

### A. The $H_2^+$ case

An initial gaseous sample of neutral  $H_2$  in thermal equilibrium at  $300 \text{ K}$  will be a mixture of 25% in  $I = 0$  and

75% in  $I = 1$ , the values arising from nuclear spin statistics (1 vs 3 nuclear spin states, respectively). By electron-impact ionization followed by cold He buffer gas cooling, the sample will be turned into a mixture of 25% para- $\text{H}_2^+$  in  $N = 0$  and 75% ortho- $\text{H}_2^+$  in  $N = 1$ , since the nuclear spin state is not affected by the ionization or the collisions with He. The  $\text{H}_2^+$  molecules are then spread over six quantum states (ignoring Zeeman substructure), with 25% in the  $N = 0$  single quantum state and 25% in the  $N = 1, J = 5/2$  single quantum state.

For a deterministic preparation of a single quantum state, we suggest the following nonoptical approach: nowadays it is routinely possible to convert neutral  $\text{H}_2$  into nearly 100% para- $\text{H}_2$  by a paramagnetic catalyst at 20 K. This gas can be used in the experiment. During subsequent electron-impact ionization the nuclear spin state is expected to be preserved, leading to nearly pure para- $\text{H}_2^+$ , which is then rotationally cooled to close to 100% in  $N = 0$ , which is a single quantum state. This represents deterministic preparation of a single quantum state by nonoptical means.

It is also possible to prepare either pure ortho- or pure para- $\text{H}_2^+$  by destroying selectively the other species by a  $1 + 1'$  resonance-enhanced multiphoton dissociation (REMPD) laser process, where the first photon is resonant with a suitable rovibrational (electric quadrupole or Raman) transition, and the second can be at the easily available wavelength 266 nm (Fig. 1). The proton fragment resulting from REMPD can be subsequently ejected from the trap. This “nuclear purification” can be extended such that only one desired hyperfine state remains in the trap. We now discuss two specific cases, deemed to be relevant to ultrahigh precision spectroscopy of  $\text{H}_2^+$ . In the following,  $F$  and  $J$  denote the total spin and total angular momentum quantum numbers, respectively, arising as follows:  $\mathbf{F}$  is the sum of nuclear spin  $\mathbf{I}$  and electron spin  $\mathbf{s}_e$ , and  $\mathbf{J}$  is the sum of  $\mathbf{F}$  and rotational angular momentum  $\mathbf{N}$ .

(1) Preparation of para- $\text{H}_2^+$ . After buffer gas cooling of a para-ortho mixture, para- $\text{H}_2^+$  is present in a single (disregarding Zeeman degeneracy) internal state  $\psi_{0,0|0,1/2,1/2} = |v = 0, N = 0, I = 0, F = 1/2, J = 1/2\rangle$  (blue semicircle in Fig. 1). Undesired ortho- $\text{H}_2^+$  molecules are in the five hyperfine states  $\psi_{0,1|1,1/2,J=(1/2,3/2)}$  and  $\psi_{0,1|1,3/2,J=(1/2,3/2,5/2)}$ . These molecules are removed by laser vibrational excitation of electric quadrupole transitions (selection rules  $\Delta L = 0, \pm 2$ ,  $\Delta J = 0, \pm 1, \pm 2$ ,  $J + J' \geq 2$ ), e.g., to the states  $\psi_{1,1|1,F'=F,J'=3/2}$  and  $\psi_{1,1|1,F'=F,J'=5/2}$ , respectively, followed by photodissociation at 266 nm. The frequencies of the necessary five vibrational transitions (blue and blue-red-dashed arrows in the figure) lie within 97 MHz, and can be excited sequentially by a single quantum cascade laser at  $4.81 \mu\text{m}$ .

(2) Preparation of ortho- $\text{H}_2^+$ . Similarly, the single state  $\psi_{0,1|1,1/2,3/2}$  of ortho- $\text{H}_2^+$  (red semicircle) is obtained by (i) vibrationally exciting the undesired para- $\text{H}_2^+$  molecules by a quantum cascade laser at  $4.58 \mu\text{m}$  on the transition  $\psi_{0,0|0,1/2,1/2} \rightarrow \psi_{1,2|0,1/2,3/2}$  (red arrow), (ii) vibrationally exciting the other four undesired ortho- $\text{H}_2^+$  spin states,  $\psi_{0,1,1|1,3/2,J} \rightarrow \psi_{1,1|1,3/2,5/2}$  and  $\psi_{0,0|1,1/2,1/2} \rightarrow \psi_{1,1|1,1/2,3/2}$ , at  $4.81 \mu\text{m}$  (blue-red-dashed arrows), all followed by UV-induced dissociation from the  $v = 1$  levels. During these excitations, the desired state  $\psi_{0,1|1,1/2,3/2}$  remains unaffected, because the laser frequency is detuned by  $-19.7$  MHz or further, which significantly exceeds the Doppler half linewidth

of the transition when the ions are sympathetically cooled, 1.6 MHz for a secular temperature 10 mK. Note that even if pure ortho- $\text{H}_2$  were employed as start gas, REMPD is still required for generating a single quantum state.

Three of the purification transitions mentioned above have also been proposed as transitions of metrological interest [1,16]. We see that two midinfrared lasers suffice for state preparation and spectroscopy. Purification of other spin states is in principle feasible in a similar way. Finally, if one wishes to produce para- $\text{H}_2^+$  in  $N = 2$ , one may perform buffer gas cooling at approximately  $T = 90$  K, followed by  $1 + 1'$  REMPD of those molecules that are in  $N = 0$  and  $N = 1$ .

### B. The $\text{D}_2^+$ case

In thermal equilibrium at 300 K, 1/3 of a  $\text{D}_2$  ensemble is para ( $I = 1$  with three nuclear Zeeman substates; odd  $N$ ), and 2/3 is ortho ( $I = 0, 2$  with six nuclear Zeeman substates; even  $N$ ). This ratio is expected to be maintained after electron-impact ionization and after buffer gas cooling. While ortho- $\text{D}_2^+$  will be cooled into the  $N = 0$  state by cold He, it still has two nuclear “species”  $I = 0, 2$ . Thus, preparation of ortho- $\text{D}_2^+$  in a single quantum state is more complicated than for the para- $\text{H}_2^+$  case, where there is only a single value  $I = 0$ . In fact, the  $N = 0$  state of ortho- $\text{D}_2^+$  possesses three quantum states  $\psi_{0,0|0,1/2,1/2}$ ,  $\psi_{0,0|2,F=(3/2,5/2),J=F}$  (energetically split by the nuclear-spin–electron-spin interaction), compared to a single one in para- $\text{H}_2^+$ .

Para- $\text{D}_2^+$  will eventually be cooled into the  $N = 1$  state, which possesses five quantum states  $\psi_{0,1|1,1/2,J=(1/2,3/2)}$ ,  $\psi_{0,1|1,3/2,J=(1/2,3/2,5/2)}$ .

Thus, starting from a thermal ensemble of  $\text{D}_2$ , after rotational cooling, the largest fractional population in a single quantum state is 1/3, in the ortho-state  $\psi_{0,0|2,5/2,5/2}$ . Preparation of a single quantum state should be possible using a REMPD-based purification similar to that described for  $\text{H}_2^+$ .

Today, it is technically well feasible to generate nearly pure ortho- $\text{D}_2$  and approximately 80%-enriched para- $\text{D}_2$  gas, similar to the  $\text{H}_2$  case [49]. While their use in rotational cooling is favorable, the additional procedure of REMPD will nevertheless be necessary if the preparation of a single quantum state is required, both for the  $N = 0$  and for the  $N = 1$  target rotational level.

## VI. PRESENT CONCLUSIONS

In the present work we have computed *ab initio* the rotationally and in part spin-state-resolved elastic and inelastic cross sections for two of the simplest nonreactive molecule-neutral-atom collisions,  $\text{H}_2^+(v = 0, N) + \text{He} \rightarrow \text{H}_2^+(v = 0, N') + \text{He}$  and  $\text{D}_2^+(v = 0, N) + \text{He} \rightarrow \text{D}_2^+(v = 0, N') + \text{He}$ . We found the rotational cooling rate coefficients to be of similar size as those for vibrational cooling. In a complete picture, a sample of initially rotationally and vibrationally excited MHI made to interact with cold He buffer gas will undergo the concurrent processes of vibrationally excited ion destruction, vibrational cooling, and rotational cooling. We computed that for both  $\text{H}_2^+$  and  $\text{D}_2^+$  initially in  $v = 0$ , complete rotational cooling into the rotational ground state is possible already for a moderately low collisional temperature of 20 K ( $T_{\text{He}} = 60$

and 40 K for  $\text{H}_2^+$  and  $\text{D}_2^+$ , respectively) within a time of approximately 40 s for a He density of  $10^9 \text{ cm}^{-3}$ . Here the rotational ground state is specific to the particular total nuclear spin  $I$  of the MHI. For molecules initially in  $v = 1, 2$ , more relaxation channels exist, but the cooling time is expected to be similar.

Two approaches were presented for achieving single-quantum state preparation of homonuclear MHIs: starting with catalytically produced pure para- $\text{H}_2$ , or removing undesired hyperfine states by hyperfine-state-resolved, stepwise photodissociation. Such controlled laser dissociation is always required for  $\text{D}_2^+$  single quantum state preparation, due to its richer spin structure.

Using an appropriate cryogenic trap apparatus, the cooling, photodissociation, and collision-free times can be made compatible with the duration of experimental spectroscopy

protocols. On the whole, we find that because of its relative simplicity, cryogenic buffer gas cooling of homonuclear MHIs by helium appears as an attractive approach for enabling next-generation spectroscopy experiments on these fundamental quantum systems. We believe that the basic concepts of the present analysis are applicable also to other homonuclear molecular ion species.

## ACKNOWLEDGMENTS

This work has been partially funded by FP7-2013-ITN “COMIQ” (Grant No. 607491) and by DFG project Schi 431/21-1. We thank S. Schlemmer and O. Asvany for stimulating discussions on reactions. The Innsbruck group also thanks the Austrian Science Fund FWF, Project No. P27047-N20.

- 
- [1] S. Schiller, D. Bakalov, and V. I. Korobov, Simplest Molecules As Candidates for Precise Optical Clocks, *Phys. Rev. Lett.* **113**, 023004 (2014).
- [2] J.-P. Karr,  $\text{H}_2^+$  and  $\text{HD}^+$ : Candidates for a molecular clock, *J. Mol. Spectrosc.* **300**, 37 (2014).
- [3] J. C. J. Koelemeij, B. Roth, A. Wicht, I. Ernsting, and S. Schiller, Vibrational Spectroscopy of  $\text{HD}^+$  with 2-ppb Accuracy, *Phys. Rev. Lett.* **98**, 173002 (2007).
- [4] U. Bressel, A. Borodin, J. Shen, M. Hansen, I. Ernsting, and S. Schiller, Manipulation of Individual Hyperfine States in Cold Trapped Molecular Ions and Application to  $\text{HD}^+$  Frequency Metrology, *Phys. Rev. Lett.* **108**, 183003 (2012).
- [5] J. Biesheuvel, J.-P. Karr, L. Hilico, K. S. E. Eikema, W. Ubachs, and J. C. J. Koelemeij, Probing QED and fundamental constants through laser spectroscopy of vibrational transitions in  $\text{HD}^+$ , *Nat. Commun.* **7**, 10385 (2016).
- [6] S. Schiller, M. Hansen, S. Alighanbari, C. Wellers, I. Kortunov, I. Ernsting, I. Sivarajah, K. Brown, D. Bakalov, and V. Korobov, Prospects for ultra-precise spectroscopy of the simplest molecules, in *Spectroscopy and Applications of Cold Molecular Ions*, Bad Honnef, 15–18 June 2015.
- [7] K. B. Jefferts, Hyperfine Structure in the Molecular Ion  $\text{H}_2^+$ , *Phys. Rev. Lett.* **23**, 1476 (1969).
- [8] A. D. J. Critchley, A. N. Hughes, and I. R. McNab, Direct Measurement of a Pure Rotation Transition in  $\text{H}_2^+$ , *Phys. Rev. Lett.* **86**, 1725 (2001).
- [9] M. Beyer and F. Merkt, Observation and Calculation of the Quasibound Rovibrational Levels of the Electronic Ground State of  $\text{H}_2^+$ , *Phys. Rev. Lett.* **116**, 093001 (2016).
- [10] A. Carrington, C. A. Leach, R. E. Moss, T. C. Steimle, M. R. Viant, and Y. D. West, Microwave electronic spectroscopy, electric field dissociation and photofragmentation of the  $\text{H}_2^+$  ion, *J. Chem. Soc., Faraday Trans.* **89**, 603 (1993).
- [11] A. Carrington, C. A. Leach, A. J. Marr, R. E. Moss, C. H. Pyne, and T. C. Steimle, Microwave spectra of the  $\text{D}_2^+$  and  $\text{HD}^+$  ions near their dissociation limits, *J. Chem. Phys.* **98**, 5290 (1993).
- [12] C. Haase, M. Beyer, C. Jungen, and F. Merkt, The fundamental rotational interval of para- $\text{H}_2^+$  by MQDT-assisted Rydberg spectroscopy of  $\text{H}_2$ , *J. Chem. Phys.* **142**, 064310 (2015).
- [13] V. I. Korobov, L. Hilico, and J. P. Karr, Theoretical transition frequencies beyond 0.1 ppb accuracy in  $\text{H}_2^+$ ,  $\text{HD}^+$ , and antiprotonic helium, *Phys. Rev. A* **89**, 032511 (2014).
- [14] P. Blythe, B. Roth, U. Fröhlich, H. Wenz, and S. Schiller, Production of Ultracold Trapped Molecular Hydrogen Ions, *Phys. Rev. Lett.* **95**, 183002 (2005).
- [15] T. Schneider, B. Roth, H. Duncker, I. Ernsting, and S. Schiller, All-optical preparation of molecular ions in the rovibrational ground state, *Nat. Phys.* **6**, 275 (2010).
- [16] J.-P. Karr, S. Patra, J. Koelemeij, J. Heinrich, N. Silltoe, A. Douillet, and L. Hilico, Hydrogen molecular ions: New schemes for metrology and fundamental physics tests, *J. Phys. Conf. Ser.* **723**, 012048 (2016).
- [17] J.-P. Karr, A. Douillet, and L. Hilico, Photodissociation of trapped  $\text{H}_2^+$  ions for REMPD spectroscopy, *Appl. Phys. B* **107**, 1043 (2012).
- [18] M. A. O’Halloran, S. T. Pratt, P. M. Dehmer, and J. L. Dehmer, Photoionization dynamics of  $\text{H}_2\text{C}^1\Pi_u$ : Vibrational and rotational branching ratios, *J. Chem. Phys.* **87**, 3288 (1987).
- [19] J.-P. Karr, F. Bielsa, A. Douillet, J. P. Gutierrez, V. I. Korobov, and L. Hilico, Vibrational spectroscopy of  $\text{H}_2^+$ : Hyperfine structure of two-photon transitions, *Phys. Rev. A* **77**, 063410 (2008).
- [20] A. Dzhonson, D. Gerlich, E. J. Bieske, and J. P. Maier, Apparatus for the study of electronic spectra of collisionally cooled cations: para-dichlorobenzene, *J. Mol. Structure* **795**, 93 (2006).
- [21] O. V. Boyarkin, S. R. Mercier, A. Kamariotis, and T. R. Rizzo, Electronic spectroscopy of cold, protonated tryptophan and tyrosine, *J. Am. Chem. Soc.* **128**, 2816 (2006).
- [22] O. Asvany, E. Hugo, F. Müller, F. Kühnemann, S. Schiller, J. Tennyson, and S. Schlemmer, Overtone spectroscopy of  $\text{H}_2\text{D}^+$  and  $\text{D}_2\text{H}^+$  using laser induced reactions, *J. Chem. Phys.* **127**, 154317 (2007).
- [23] S. Schlemmer, T. Kuhn, E. Lescop, and D. Gerlich, Laser excited  $\text{N}_2^+$  in a 22-pole ion trap: experimental studies of rotational relaxation processes, *Int. J. Mass Spectrom.* **185-187**, 589 (1999).
- [24] D. Hauser, S. Lee, F. Carelli, S. Spieler, O. Lakhmanskaya, E. S. Endres, S. S. Kumar, F. Gianturco, and R. Wester, Rotational state-changing cold collisions of hydroxyl ions with helium, *Nat. Phys.* **11**, 467 (2015).



- [25] L. P. Theard and W. T. Huntress, Ion-molecule reactions and vibrational deactivation of  $\text{H}_2^+$  ions in mixtures of hydrogen and helium, *J. Chem. Phys.* **60**, 2840 (1974).
- [26] A. K. Hansen, O. O. Versolato, L. Klosowski, S. B. Kristensen, A. Gingell, M. Schwarz, A. Windberger, J. Ullrich, J. R. C. Lopez-Urrutia, and M. Drewsen, Efficient rotational cooling of Coulomb-crystallized molecular ions by a helium buffer gas, *Nat. Lett.* **508**, 76 (2014).
- [27] R. G. DeVoe, Power-law Distributions in a Trapped Ion Interacting with a Classical Buffer Gas, *Phys. Rev. Lett.* **102**, 063001 (2009).
- [28] O. Asvany and S. Schlemmer, Numerical simulations of kinetic ion temperature in a cryogenic linear multipole trap, *Int. J. Mass Spectrom.* **279**, 147 (2009).
- [29] C. Zipkes, L. Ratschbacher, C. Sias, and M. Köhl, Kinetics of a single trapped ion in an ultracold buffer gas, *New J. Phys.* **13**, 053020 (2011).
- [30] B. Höltekemeyer, P. Veckesser, H. López-Carrera, and M. Weidemüller, Buffer Gas Cooling of a Single Ion in a Multipole Radio-Frequency Trap Beyond the Critical Mass Ratio, *Phys. Rev. Lett.* **116**, 233003 (2016).
- [31] C. B. Zhang, D. Offenber, B. Roth, M. A. Wilson, and S. Schiller, Molecular-dynamics simulations of cold single-species and multispecies ion ensembles in a linear Paul trap, *Phys. Rev. A* **76**, 012719 (2007).
- [32] B. Roth and S. Schiller, *Cold Molecules* (Taylor and Francis, London, 2009), pp. 651–704.
- [33] F. von Busch and G. H. Dunn, Photodissociation of  $\text{H}_2^+$  and  $\text{D}_2^+$ : Experiment, *Phys. Rev. A* **5**, 1726 (1972).
- [34] Y. Weijun, R. Alheit, and G. Werth, Vibrational population of  $\text{H}_2^+$  after electroionization of thermal  $\text{H}_2$ , *Z. Phys. D* **28**, 87 (1993).
- [35] T. Glenwinkel-Meyer and D. Gerlich, Single and merged beam studies of the reaction  $\text{H}_2^+(v = 0, 1; j = 0, 4) + \text{H}_2 \rightarrow \text{H}_3^+ + \text{H}$ , *Isr. J. Chem.* **37**, 343 (1997).
- [36] F. Mrugała, V. Špirko, and W. P. Kraemer, Radiative association of  $\text{HeH}_2^+$ , *J. Chem. Phys.* **118**, 10547 (2003).
- [37] S. Brünken, L. Kluge, A. Stoffels, J. Pérez-Riós, and S. Schlemmer, Rotational state-dependent attachment of He atoms to cold molecular ions: An action spectroscopic scheme for rotational spectroscopy, *J. Mol. Spectrosc.* **332**, 67 (2016).
- [38] T.-S. Chu, R.-F. Lu, K.-L. Han, X.-N. Tang, H.-F. Xu, and C. Y. Ng, A time-dependent wave-packet quantum scattering study of the reaction  $\text{H}_2^+(v = 0 - 2, 4, 6; j = 1) + \text{He} \rightarrow \text{HeH}^+ + \text{H}$ , *J. Chem. Phys.* **122**, 244322 (2005).
- [39] C. Ramachandran, D. D. Fazio, S. Cavalli, F. Tarantelli, and V. Aquilanti, Revisiting the potential energy surface for the  $\text{He} + \text{H}_2^+ \rightarrow \text{HeH}^+ + \text{H}$  reaction at the full configuration interaction level, *Chem. Phys. Lett.* **469**, 26 (2009).
- [40] M. Wernli, E. Bodo, and F. A. Gianturco, Rotational cooling efficiency upon molecular ionization: The case of  $\text{Li}_2(a^3\Sigma_u^+)$  and  $\text{Li}_2(X^2\Sigma_g^+)$  interacting with  $^4\text{He}$ , *Eur. Phys. J. D* **45**, 267 (2007).
- [41] M. Tacconi, F. A. Gianturco, E. Yurtsever, and D. Caruso, Cooling and quenching of  $^{24}\text{MgH}^+(X^1\Sigma^+)$  by  $^4\text{He}(^1\text{S})$  in a Coulomb trap: A quantum study of the dynamics, *Phys. Rev. A* **84**, 013412 (2011).
- [42] J. Pérez-Riós and F. Robicheaux, Rotational relaxation of molecular ions in a buffer gas, *Phys. Rev. A* **94**, 032709 (2016).
- [43] M. H. Alexander, Rotationally inelastic collisions between a diatomic molecule in a  $^2\Sigma^+$  electronic state and a structureless target, *J. Chem. Phys.* **76**, 3637 (1982).
- [44] G. C. Corey and F. R. McCourt, Inelastic differential and integral cross sections for  $^{2S+1}\Sigma$  linear molecule  $^1\text{S}$  atom scattering: The use of Hund's case (b) representation, *J. Phys. Chem.* **87**, 2723 (1983).
- [45] M. H. Alexander, J. E. Smedley, and G. C. Corey, On the physical origin of propensity rules in collisions involving molecules in  $^2\Sigma$  electronic states, *J. Chem. Phys.* **84**, 3049 (1986).
- [46] M. Hernández Vera, S. Schiller, R. Wester, and F. A. Gianturco, Rotationally inelastic cross sections, rates and cooling times for para- $\text{H}_2^+$ , ortho- $\text{D}_2^+$  and  $\text{HD}^+$  in cold helium gas, *Eur. Phys. J. D* (unpublished).
- [47] D. López-Durán, E. Bodo, and F. A. Gianturco, ASPIN: An all-spin code for atom-molecule rovibrationally inelastic cross sections, *Comput. Phys. Commun.* **179**, 821 (2008).
- [48] M. Hernández Vera, F. A. Gianturco, R. Wester, H. da Silva, Jr., O. Dulieu, and S. Schiller, Rotationally inelastic collisions of  $\text{H}_2^+$  ions with He buffer gas: Computing cross sections and rates, *J. Chem. Phys.* **146**, 124310 (2017).
- [49] H. Imao, K. Ishida, N. Kawamura, T. Matsuzaki, Y. Matsuda, A. Toyoda, P. Strasser, M. Iwasaki, and K. Nagamine, Preparation of ortho-para ratio controlled  $\text{D}_2$  gas for muon-catalyzed fusion, *Rev. Sci. Instrum.* **79**, 053502 (2008).